PHYSICAL REVIEW E **75**, 055301(R) (2007)

Dynamical states of a mobile heat blanket on a thermally convecting fluid

Jin-Qiang Zhong[1] and Jun Zhang[1,2,*]

[1]*Department of Physics and Center for Soft Matter Research, New York University, 4 Washington Place, New York, New York 10003, USA*

[2]*Applied Mathematics Laboratory, Courant Institute of Mathematical Sciences, New York University, 251 Mercer Street, New York, New York 10012, USA*

(Received 2 October 2006; published 9 May 2007)

We experimentally study the dynamical states of a freely moving, floating heat blanket that is coupled with a thermally convecting fluid. This floating boundary modifies the large-scale flow pattern in the bulk and destabilizes the coupled system, leading to spontaneous oscillations. As the moving boundary exceeds a critical size, the system makes a transition from an oscillatory state to a weakly confined state, in which the moving boundary executes only small excursions in response to random bypassing thermal plumes. To explain the observed states and transition, we provide a low-dimensional model that appears to capture the underlying mechanism of this coupled system.

DOI: 10.1103/PhysRevE.75.055301 PACS number(s): 47.27.te, 47.20.Bp, 91.45.Fj

In the classical Rayleigh-Bénard thermal convection experiment, a fluid enclosed within a rigid container is heated from below and cooled at the top. In the presence of gravity, the resultant buoyancy forces cause the fluid to convect, allowing heat to transfer efficiently across the cell. Because this system can be rigorously defined by choosing a known fluid and precise boundary conditions, it has become a prototypical environment for studying complex dynamical systems [1–4]. In the classical setting, the container walls are rigid and do not respond to the rich dynamics exhibited by the moving fluid. We now pose the following questions: What would happen if one of the boundaries was mobile and could be driven by viscous stresses generated by the convecting fluid? Would this added degree of freedom give rise to more complex behavior in the coupled system?

Our previous experiments demonstrated the basic effect that a single floating boundary over a thermally convective fluid could be driven into nearly periodic oscillations [5,6]. There, a mobile boundary exerts a heat-blocking effect, which slowly modifies large-scale flow structures in the fluid bulk. The motion of the floating boundary is itself subject to the viscous stresses from the underlying fluid. This mutual feedback yields large-scale oscillations, which coexist with finely scaled, time-dependent turbulent flows.

One related phenomenon in nature is that of continental drift. Earlier studies [7] have suggested that an upper boundary over a thermally convecting fluid can be regarded as a model continent floating over the Earth's mantle. The geophysical process by which continents modify large-scale flows in the mantle is quite similar to how the free boundary affects the convective fluid in our experiments. Elaborate numerical simulations [8,9] have shown that the drag from the convective mantle drives continents to collide or disperse, creating restless motion along the surface of the Earth.

In this work we study the effects of floating boundary size on the coupled dynamics, and show that as the floater size is increased, its dynamics changes from oscillatory to intermittent to confined states. Further, we provide a simple model that explains these observations.

Shown in Fig. 1, our thermal convection cell, filled with water, is 60 cm long, 7.8 cm (W) wide, and 11.3 cm (H) in height. Only the central section (D, 36.5 cm in length) of the convection cell is used for our study. A floating plastic plate of thickness 0.6 cm partially covers the free fluid surface. The width (w) of the plate spans 88% of the width (W) of the convection cell. The length (d) of the plate is changed from $0.2D$ to $0.8D$ incrementally. Between the two end walls, the floating plate can freely move along the long axis of the convection cell, as it responds to viscous forces from the

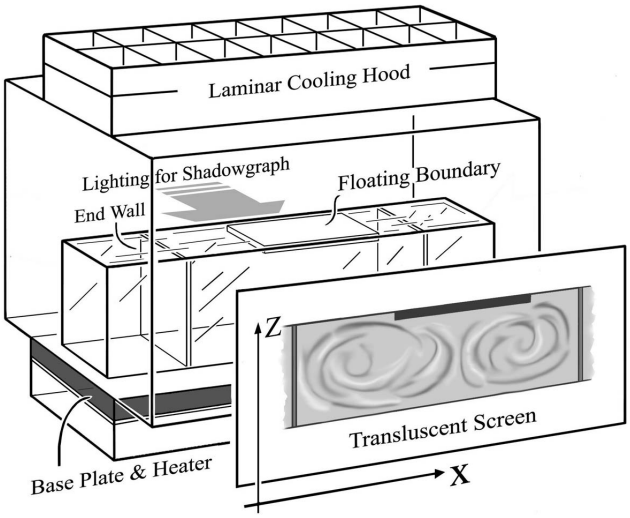

FIG. 1. A thermal convection cell containing water is heated from below and cooled at the free surface in a laminar hood. It is partially covered by a freely moving floating boundary. By inserting internal partitions—the two end walls—we use only the middle section of the convection cell; this much reduces lateral heat exchange. On top of the laminar hood, a series of cooling fans and flow diffusers are regularly arranged (not shown). A shadowgraph, projected by a nearly parallel beam of light sent through the convection cell from behind, reveals the flow structure on the translucent screen.

*Electronic address: jun@cims.nyu.edu

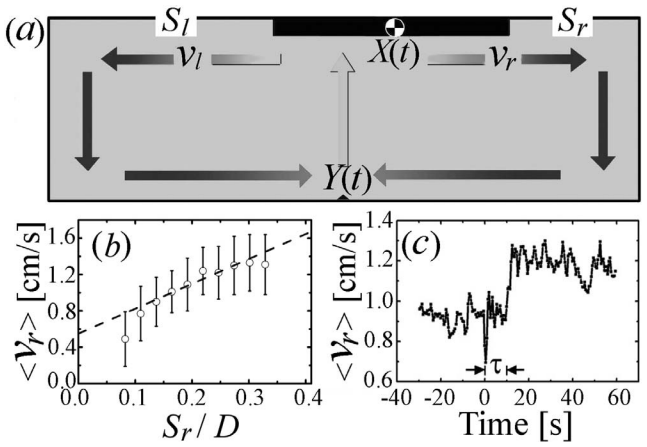

FIG. 2. (a) The fluid-loop model used in our analysis (see text for details). The open fluid surface (S_l or S_r) affects the mean flow speed of its corresponding circulation (v_l or v_r), which increases monotonically as the exposed fluid surface widens, as shown in (b). Here, speed v_r changes as S_r is increased incrementally, by placing a floater (size $0.6D$) at different locations. The dashed line indicates the slope and the offset used in our model (v_0=0.55 cm/s and θ =0.075 s^{-1}). (c) The flow response has a delay of about 10 s. At t =0, we relocate the floating boundary (d=0.6D) so that S_r changes from 5 to 10 cm. After the delay, v_r adapts to a new value. The data shown here is an average of 30 measurements.

underlying convecting flow. The convection cell is uniformly heated from below with a dc electric heater and cooled from above using a laminar air hood. The typical temperature difference between the top and the bottom is 12.0 °C. The Rayleigh number, the dimensionless control parameter of the convective system [1], is $\mathrm{Ra}=\alpha g \Delta T H^3/\nu\kappa$, where g is the acceleration due to gravity, ΔT is the temperature difference across the top and bottom, and α, ν, and κ are the thermal expansion coefficient, the kinematic viscosity, and the thermal diffusivity of the fluid, respectively. Throughout our experiment, the Rayleigh number is fixed at 1.1×10^9, close to that of mantle convection inside the Earth [8,10], and the convection is in the turbulent regime [11].

A floating boundary on the free surface of the convecting fluid suppresses the local convective mixing of the fluid, thus reducing the vertical heat loss [12,13]. At Rayleigh number 1.1×10^9, the heat flux through the open fluid surface is about ten times higher than the flux through the floating boundary [6]. Similarly, the ratio of the heat flux through the oceanic lithosphere to the heat flux through the continental lithosphere is approximately ten [14]. Such "thermal blanketing" effect induces an upwelling flow structure in the fluid beneath, as shown in Fig. 2(a). Two large-scale circulations, separated by the upwelling, emerge and compete for the available space within the cell. This system is unstable: the floating boundary lies on top of a divergent flow and will be forced away from the upwelling.

Once the floating boundary changes position, the large-scale flow reorganizes itself. After a few fluid circulations, the upwelling flow approaches below the center of the floating boundary and the net viscous driving force applied at the plate base switches direction [5,6,15]. As this process continues, the coupled system undergoes spontaneous oscillation; both the floating boundary and the flow pattern rearrange themselves in a cyclic fashion.

The first four panels of Fig. 3 show that the oscillation period becomes progressively shorter and more regular as the size of the floating boundary is increased incrementally from $0.2D$ to $0.5D$. This result shows that longer boundaries give greater thermal perturbation to the system, causing shortened periods at increased regularity.

While one might expect even faster oscillations as the size of the top boundary further increases, an unexpected state emerges. When the boundary size is greater than $0.6D$, the floater ceases oscillating between the two end walls. Instead, it appears to be trapped in the middle portion of the convection cell, making only small excursions to both sides in a seemingly random fashion. Flow visualization shows that the floating boundary lies on top of the upwelling flow and is passively driven by the randomly passing hot plumes embedded in the upwelling. The exact excursion, in direction and amplitude, of the floating boundary depends on the detailed position and size of the passing plumes. The last two time

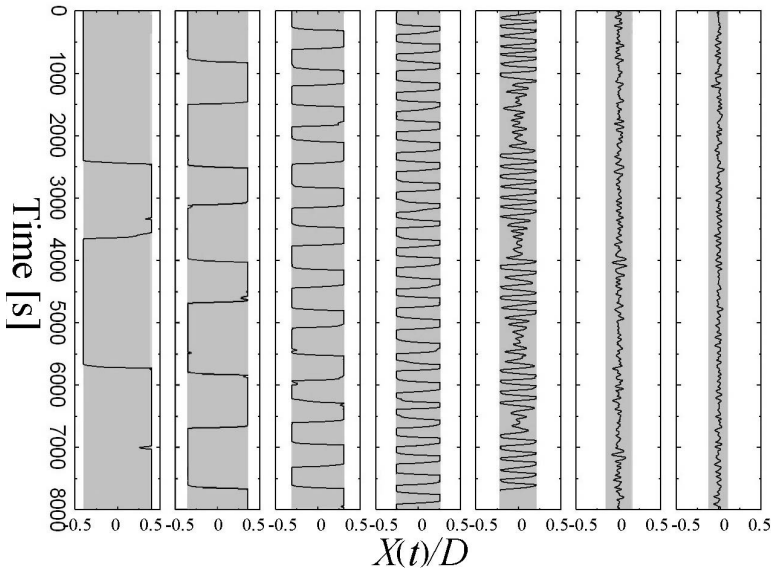

FIG. 3. Time series of the floating boundary position. An oscillatory state (panels 1–4), a trapped state (panels 6 and 7), and intermittency (panel 5) are observed as the size of the floating boundary is increased incrementally (by $0.1D$) from $0.2D$ to $0.8D$. Solid lines indicate the trajectories of the center of mass of the boundary and gray bands indicate accessible free space, $D-d$, on the surface of the convection cell.

series of Fig. 3 show such a trapped state. When the size of the boundary is increased from $0.7D$ to $0.8D$, the trapped state exhibits yet stronger confinement as the root-mean-square excursion amplitude decreases from $0.029D$ to $0.018D$. When the size of the floating boundary is at $0.6D$, intermittency between oscillation and the trapped state is observed, as seen in panel 5 of Fig. 3.

To understand this puzzling transition, we find the following clue. The circulation speed of a large-scale circulation, measured by a laser Doppler velocimetry (LDV), is directly related to the area of the open fluid surface exposed to cooling. Efficient cooling at the surface provokes greater emission of downwelling cold plumes, which drives the local flow circulation faster. Figure 2(b) shows the horizontal component of the flow speed, v_i, within an eddy versus the linear span of the open fluid surface, S_i, as indicated in Fig. 2(a), where i stands for left or right. The flow speed increases monotonically as the area of the open surface increases. Each data point shown in Fig. 2(b) is a result of a 5 min average of the flow speed; the error bars show the root-mean-square fluctuation. We also observe that the flow speed does not change immediately as the floating boundary has changed to a new location. Such response takes place with a short time delay, $\tau=10\pm1$ s, as shown in Fig. 2(c).

It is quite challenging to fully simulate the Navier-Stokes dynamics of this system since it includes a moving boundary coupled with turbulent thermal convection. Instead, as shown below, we consider a phenomenological approach.

We carry out a fluid-loop model as illustrated in Fig. 2(a). In Rayleigh-Bénard convection, this type of model has been used to investigate the large-scale flow response to heterogeneous boundary conditions [16]. In our system, the net viscous force acting on the floating boundary results from the two competing large-scale circulations. Immediately outside of the viscous boundary layer, the horizontal component of the flow speed within each circulation are v_l and v_r. We assign the geometric center of the cell as the origin of the coordinate and focus on the following: $X(t)$, the displacement of the floating boundary from the origin, and $Y(t)$, the horizontal position of the upwelling.

Let us examine the shape of the potential curve seen by the floating boundary. Assuming now that the upwelling flow remains in the middle of the cell, or $Y(t)=0$, we calculate the net viscous force acting on the floating boundary, located at X. The partial area of the boundary that lies on top of each eddy is $A_{r,l}=w(d/2\pm X)$. We assume the relationship between the circulation speed and the exposed fluid surface has a simple form $v_i=v_0+\theta S_i$, where v_0 is the offset and θ is the coefficient shown in Fig. 2(b). The viscous driving forces become $F_{r,l}=\eta A_{r,l}(\partial v_{r,l}/\partial Z)\approx \eta w(d/2\pm X)[v_0+\theta(D/2-d/2\mp X)]/\lambda$ where η is the viscosity of the fluid and λ is the thickness of the viscous boundary layer next to the plate. The net force applied on the free boundary is then $F_{net}=F_r-F_l\approx -2\eta w\lambda^{-1}[\theta(d-D/2)-v_0]X=KX$ which is proportional to the displacement, X. At fixed Rayleigh number, the above coefficient K depends only on the size of the floating boundary, d. For sufficiently large d, at least greater than $D/2$, K becomes negative and the floating boundary thus experiences a concave potential. With finite dissipation, this situation corresponds to a stable state since any finite X will decay to zero. For small top boundary sizes, however, K is positive thus the system is unstable. Changing the size of the floating boundary changes the shape of the potential it experiences, from convex for small d to concave for large d.

The reasoning above explains the transition between the two states when the upwelling is in a fixed position. However, as we observed in the experiment, the upwelling effectively follows the top boundary. The consequent interaction between the time-dependent flow structure and the free boundary can be simulated using a one-dimensional, phenomenological model. In the model, the convective flow exerts viscous shear force at the base of the plate and causes it to move. The moving boundary experiences a resistance at its four edges that is proportional to its speed. Since the motion is overdamped [15], the resistance balances with the driving force

$$\gamma\eta\dot{X}=\frac{\eta w}{\lambda}\int_d[v(x,t)-\dot{X}]dx=\frac{\eta w}{\lambda}\left[\int_d v(x,t)dx-\dot{X}d\right] \tag{1}$$

and the flow speed for each circulation has the form

$$v_i(t)=v_0+\theta S_i(t-\tau)\quad (i=l,r), \tag{2}$$

where γ is a damping coefficient, a geometric factor of the rectangular plate, which is related to the Stokesian resistance [17].

The top boundary attracts the upwelling flow. Any portion of the top boundary contributes to the migrating speed of the upwelling, $\dot{Y}(t)$. Along the length d of the floating boundary, function $G(x,Y)=\beta(x-Y)$ denotes such a contribution, to $\dot{Y}(t)$, from a segment of unit length at position x. This function is proportional to the horizontal distance $(x-Y)$ between the segment and the upwelling flow. Factor β is the proportionality constant. Then we have

$$\dot{Y}=\int_d G(x,Y)dx=\beta\int_d(x-Y)dx=d\beta(X-Y). \tag{3}$$

By combining the above three equations, we obtain the following coupled equations for the position of the top boundary and the position of the upwelling flow:

$$\dot{X}(t)=a(d)[X(t)-Y(t)]+b(d)X(t-\tau),$$
$$\dot{Y}(t)=c(d)[X(t)-Y(t)], \tag{4}$$

where $a(d)=[2v_0+\theta(D-d)]/(d+\gamma\lambda/w)$, $b(d)=-\theta d/(d+\gamma\lambda/w)$ and $c(d)=\beta d$. Further, there are spatial constraints from the two end walls: $|X(t)|\leq(D-d)/2$ and $|Y(t)|\leq D/2$. This coupled system is now described as a linear delay differential equation.

Besides constants v_0, θ, and τ [Figs. 2(b) and 2(c)], our model also needs $\gamma\lambda/w$ and β to be estimated from the experiment. In the oscillatory state near the critical point, $d=0.6D$, the maximum moving speed of the floating boundary is measured to be one-quarter of that of the flow ($\dot{X}_{max}\approx 0.25v$), when the boundary is subject to a single circula-

tion. From Eq. (1), we have $\dot{X}=(v_r A_r - v_l A_l)/(wd+\gamma\lambda)$ and $\dot{X}_{max} \approx 0.6Dv/(0.6D+\gamma\lambda/w)$. Thus we have the estimate $\gamma\lambda/w \approx 1.8D$. The proportional constant β can be estimated using the time it takes for the upwelling to migrate over a finite distance. From Eq. (3): $\dot{Y}=d\beta(X-Y)$, we can estimate that $\beta \approx 0.017D^{-1}$ s^{-1}. In short, coefficients ($\gamma\lambda/w$, v_0, θ, β, and τ) are determined to be ($1.8D$, $0.015D$ s^{-1}, 0.075 s^{-1}, $0.017D^{-1}$ s^{-1}, and 10 s).

Varying the size of the floating boundary, d (the only control parameter in the model), we find that this system undergoes a Hopf bifurcation [18] at the critical value $d_c = 0.576D$, exhibiting an oscillatory state as $d<d_c$ or a trapped state when $d>d_c$. Equation (4) can be solved analytically [15]. Its numerical solutions are shown in Fig. 4 for different top boundary sizes (from $0.3D$ to $0.75D$). The first two panels show that the top boundary oscillates together with the upwelling flow, bounded within the convection cell.

In the last two panels of Fig. 4, a trapped state appears after a few decaying oscillations, as any initial offset of the top boundary converges to zero. A comparison between cases when $d=0.65D$ and $d=0.75D$ indicates that a larger floating boundary experiences stronger confinement, leading to faster convergence. Since our model contains no noise component (flow speed fluctuation, small random shift of flow pattern), the result shows no random excursions in the trapped state.

At the critical size, however, the top boundary sustains a marginal oscillation, barely touching the end walls (Fig. 4, panel 3). We find, from additional experiment, that changing Ra alters the value of the critical size d_c. In the model, if we set $\tau=0$, d_c shifts to $0.532D$. The effects of both Ra and τ are discussed elsewhere [15].

The interactions between moving bodies and fluid flows are difficult to understand quantitatively yet are ubiquitous in nature and technology. Our system is relatively simple: a free moving thermal blanket interacting with its induced flow structure. The results from our simple model agree quite well with the experimental observations. The model also explains, the existence of the oscillatory state as also observed previously [5,6]. The intermittency between the oscillatory and trapped states shown in Fig. 3 (panel 5) is yet to be understood.

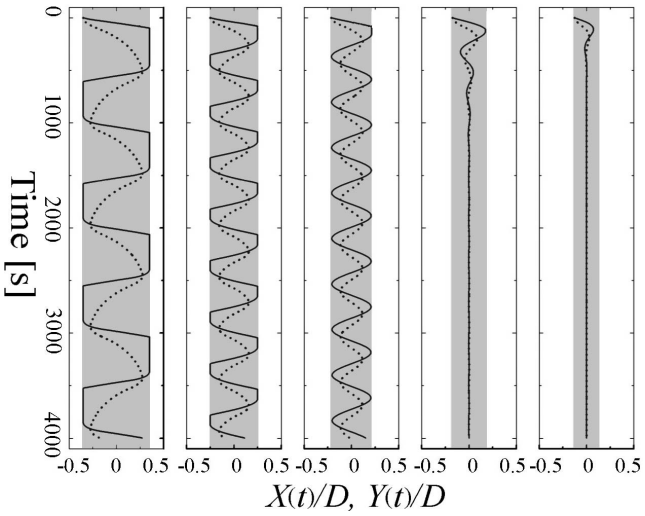

FIG. 4. The numerical results. The time series of the floating boundary [$X(t)$, solid line] and the position of the upwelling flow [$Y(t)$, dashed line] show oscillatory and trapped states. Gray bands show accessible space ($D-d$) for the floating boundary on top of the cell. From left to right, d/D is 0.3, 0.5, 0.576, 0.65, and 0.75, respectively.

We thank M. Shelley, A. Libchaber, B. Liu, and M. Harp for helpful discussions. This work was supported by the Department of Energy (Grant No. DE-FG0288ER25053).

[1] L. Rayleigh, Philos. Mag. **32**, 529 (1916).
[2] M. C. Cross and P. C. Hohenberg, Rev. Mod. Phys. **65**, 851 (1993).
[3] S. Grossmann and D. Lohse, J. Fluid Mech. **407**, 27 (2000).
[4] L. P. Kadanoff, Phys. Today **54**, 34 (2001).
[5] J. Zhang and A. Libchaber, Phys. Rev. Lett. **84**, 4361 (2000).
[6] J.-Q. Zhong and J. Zhang, Phys. Fluids **17**, 115105 (2005).
[7] J. Elder, Sci. Prog. **56**, 1 (1968); L. N. Howard, W. V. R. Malkus, and J. A. Whitehead, Geophys. Fluid Dyn. **1**, 123 (1970); J. A. Whitehead, Phys. Earth Planet. Inter. **5**, 199 (1972).
[8] M. Gurnis, Nature (London) **332**, 695 (1988).
[9] J. P. Lowman and G. T. Jarvis, Geophys. Res. Lett. **20**, 2087 (1993).
[10] D. L. Turcotte and G. Schubert, *Geodynamics* (Cambridge University Press, New York, 2002).
[11] F. Heslot, B. Castaing, and A. Libchaber, Phys. Rev. A **36**, 5870 (1987).
[12] F. H. Busse, Geophys. J. R. Astron. Soc. **52**, 1 (1978).
[13] J. P. Lowman and G. T. Jarvis, Phys. Earth Planet. Inter. **88**, 53 (1995).
[14] C. Grigné and S. Labrosse, Geophys. Res. Lett. **28**, 2707 (2001).
[15] J.-Q. Zhong and J. Zhang, Phys. Rev. E (to be published).
[16] L. Guillou and C. Jaupart, J. Geophys. Res., [Solid Earth] **100**, 24217 (1995).
[17] R. Roscoe, Philos. Mag. **40**, 338 (1949).
[18] K. L. Cooke and Z. Grossman, J. Math. Anal. Appl. **86**, 592 (1982).